Experimental and Molecular Pathology 91 (2011) 664–672

Contents lists available at SciVerse ScienceDirect

Experimental and Molecular Pathology

journal homepage: www.elsevier.com/locate/yexmp

Human hepatic stellate cell line (LX-2) exhibits characteristics of bone marrow-derived mesenchymal stem cells

Andrielle Castilho-Fernandes [a,b,*], Danilo Candido de Almeida [a,b], Aparecida Maria Fontes [a,b], Fernanda Ursoli Ferreira Melo [b], Virgínia Picanço-Castro [b], Marcela Cristina Freitas [a,b], Maristela D. Orellana [a,b], Patricia V.B. Palma [b], Perry B. Hackett [c], Scott L. Friedman [d], Dimas Tadeu Covas [a,b]

[a] Faculty of Medicine of Ribeirão Preto, Department of Clinical Medicine, University of São Paulo, Av. Bandeirantes, 3900 (6° andar do HC) Ribeirão Preto 14048-900, Brazil
[b] Center for Cell Therapy and Regional Blood Center of Ribeirão Preto, National Institute of Science and Technology in Stem Cell and Cell Therapy, Rua Tenente Catão Roxo, 2501, Ribeirão Preto 14051-140, Brazil
[c] Department of Genetics, Cell Biology, and Development, University of Minnesota, 6-160 Jackson Hall, 321 Church St. SE, Minneapolis 55455, USA
[d] Mount Sinai School of Medicine, Icahn Medical Institute, 11th Floor, Room 11-70C, 1425 Madison Avenue, NY 10029, USA

ARTICLE INFO

Article history:
Received 15 March 2011
and in revised form 2 September 2011
Available online 9 September 2011

Keywords:
Hepatic stellate cell line
LX-2
Mesenchymal stem cells
Pericytes

ABSTRACT

The LX-2 cell line has characteristics of hepatic stellate cells (HSCs), which are considered pericytes of the hepatic microcirculatory system. Recent studies have suggested that HSCs might have mesenchymal origin. We have performed an extensive characterization of the LX-2 cells and have compared their features with those of mesenchymal cells. Our data show that LX-2 cells have a phenotype resembling activated HSCs as well as bone marrow-derived mesenchymal stem cells (BM-MSCs). Our immunophenotypic analysis showed that LX-2 cells are positive for activated HSC markers (αSMA, GFAP, nestin and CD271) and classical mesenchymal makers (CD105, CD44, CD29, CD13, CD90, HLA class-I, CD73, CD49e, CD166 and CD146) but negative for the endothelial marker CD31 and endothelial progenitor cell marker CD133 as well as hematopoietic markers (CD45 and CD34). LX-2 cells also express the same transcripts found in immortalized and primary BM-MSCs (vimentin, annexin 5, collagen 1A, NG2 and CD140b), although at different levels. We show that LX-2 cells are capable to differentiate into multilineage mesenchymal cells in vitro and can stimulate new blood vessel formation in vivo. LX-2 cells appear not to possess tumorigenic potential. Thus, the LX-2 cell line behaves as a multipotent cell line with similarity to BM-MSCs. This line should be useful for further studies to elucidate liver regeneration mechanisms and be the foundation for development of hepatic cell-based therapies.

Introduction

The liver has the remarkable capacity to regenerate after tissue loss. The cellular and molecular mechanisms underlying liver regeneration involve several growth factors, cytokines, and proteases which promote the cellular proliferation in an injured area (Zimmermann, 2004). The hepatic parenchyma consists of parenchymal and non-parenchymal cells associated with sinusoids and includes hepatic stellate cells (HSCs). HSCs are engaged in several important functions under both physiological and pathological conditions (De Minicis et al., 2007). In healthy liver, quiescent HSCs are characterized by a star-like morphology, store vitamin A in lipid droplets and have a low proliferating activity. HSCs were first described by Kupffer in 1876 (Wake, 1971), and a fat-staining method used by Ito has defined these cells as "fat-storing cells" (Ito and Shibasaki, 1968). HSCs are considered pericytes of the hepatic microcirculatory system and are located in the perisinusoidal space of Disse (Atzori et al., 2009). Their multiple, long cytoplasmic protrusions run parallel to the sinusoidal endothelial wall, embrace the sinusoid, and penetrate between hepatocytes to reach neighboring sinusoids (McCuskey, 2008). Liver damage leads to activation of HSCs from a quiescent phenotype into an activated phenotype — myofibroblast-like cells. Activated HSCs lose their capacity to store vitamin A, proliferate vigorously and secrete a large amount of extra-cellular matrix, which contributes to hepatic fibrosis (Budny et al., 2007; Friedman et al., 1985; Mann and Mann, 2009).

HSCs are believed to be derived from mesenchymal origin and experimental evidence suggests that it could be derived from bone marrow-derived mesenchymal stem cells (BM-MSCs) (Friedman, 2008; Russo et al., 2006). Previous studies indicated that BM-MSCs and pericytes have a common embryonic origin; both cell types can differentiate into multilineage mesenchymal cells and acquire functions for repair and tissue maintenance (Armulik et al., 2005; Brachvogel et al., 2005; Covas

* Corresponding author at: National Institute of Science and Technology in Stem Cell and Cell Therapy, Regional Blood Center of Ribeirão Preto, HC/FMRP-USP, 2501 Tenente Catão Roxo St, Monte Alegre, 14051-140, Ribeirão Preto, São Paulo, Brazil. Fax: +55 16 2101 9309.
E-mail address: andrielle_dcf@yahoo.com (A. Castilho-Fernandes).

0014-4800/$ – see front matter © 2011 Elsevier Inc. All rights reserved.
doi:10.1016/j.yexmp.2011.09.002

et al., 2008). By serial analysis of gene expression (SAGE), Covas et al. (2008) observed that HSCs formed a consistent cluster with BM-MSCs and retinal pericytes, which indicates the close relationship of these cells. Some reports demonstrate that BM-MSCs play a major role in either generation or degradation of hepatic fibrosis, as well as in improvement liver function following liver damage (Flohr et al., 2009; Russo et al., 2006). In fact, quiescent and early activated HSCs promote extracellular matrix degradation by producing matrix metalloproteinases (Benyon and Arthur, 2001). Although liver regeneration has been studied for many years, the mechanism(s) involved are poorly understood (Alison et al., 2007). Thus, an extensive characterization of a population of HSCs is of paramount importance for understanding responses to hepatic injury.

At present, there are two main sources of HSCs, freshly isolated HSCs or HSC cell lines. However primary HSCs are scarce; they represent only about 5–8% of the cells in a normal liver. Besides, the limited access to human hepatic tissue make it difficult to use the primary HSCs (Atzori et al., 2009). Hence, immortalized cell lines have been used to overcome this problem. Although current cell lines have limited utility as clinically transplantable agents, the use of an immortalized HSC cell line should provide valuable insights into a number of aspects of HSC behavior important for development of hepatic cell-based therapies in experimental models, including engraftment, immunogenicity and efficiency of cell transplantation. The LX-2 cell line, developed by Xu et al. (2005), has been used to show the in vivo phenotype of human HSCs in order to elucidate pathways of human hepatic fibrosis and to develop antifibrotic therapies. We hypothesize that LX-2 cells have a close association with BM-MSCs. Our results showed that LX-2 cells are similar to BM-MSCs in several aspects including immunophenotypic and transcriptional properties. Our data also show that LX-2 cells are capable of differentiating into adipocytes and osteocytes in vitro and can participate in the blood vessel formation in vivo. LX-2 cells appear to not possess tumorigenic potential. Thus, LX-2 cells may be safely used for in vitro and in vivo studies of stem cell therapies for hepatic diseases.

Materials and methods

Isolation and growth of cellular types

The LX-2 cell line, a spontaneously immortalized human hepatic stellate cell, was kindly provided by Dr. Scott L. Friedman (Mount Sinai School of Medicine, New York, NY). LX-2 cells were maintained in DMEM (Life Technologies — Invitrogen, Carlsbad, CA, USA) and supplemented with 2% (v/v) FBS (Gibco — Invitrogen, Carlsbad, CA, USA). The human bone marrow stromal cell line (HBMS) was kindly provided by Dr. Dario Campana (Department of Pediatrics, University of Tennessee College of Medicine, Memphis, TN) (Mihara et al., 2003). Bone marrow-derived mesenchymal stem cells (BM-MSCs) were obtained from healthy donors and were cultured as previously described by Silva et al. (2003). Human umbilical vein endothelial cells (HUVEC) were isolated and cultured as described by Covas et al. (2008). CD133+ cells were isolated from umbilical cord blood samples as described by Bordeaux-Rego et al. (2010). All cultures were grown at 37 °C and 5% CO_2. Our studies were conducted according to ethical guidelines approved by the Regional Scientific-Ethical Committee on the Use of Human Subjects at the School of Medicine of Ribeirão Preto, University of São Paulo, Brazil. All participants signed an informed written consent.

Flow cytometry analysis

The immunophenotypic characterizations of LX-2, HBMS and BM-MSC cells were performed by flow cytometry using the following 16 monoclonal antibodies: CD73 (NT5E, 5′-nucleotidase, ecto)-FITC (fluorescein isothiocyanate) or PE (phycoerythrin), HLA-class I (major histocompatibility complex, class I)-PE [Pharmingen], CD14-PE, CD29 (ITGB1, integrin, beta 1)-PE, CD31 (HBA1, hemoglobin, alpha 1)-FITC or PE, CD34-PE, CD44-FITC or PE, CD45 (Leukocyte common antigen)-FITC or PE, CD49e (ITGA5, integrin, alpha 5)-PE, CD90 (THY1, Thy-1 cell surface antigen)-PE, CD105 (ENG, endoglin)-PE, CD106 (VCAM1, vascular cell adhesion molecule 1)-PE, CD146 (MCAM, melanoma cell adhesion molecule)-PE, CD166 (ALCAM, activated leukocyte cell adhesion molecule)-PE, HLA-class II-FITC or PE (BD Biosciences, San Jose, CA, USA). On the other hand, α-SMA (alpha-smooth muscle actin) (Sigma-Aldrich, St. Louis, MO, USA), GFAP (glial fibrillary acidic protein) (Sigma-Aldrich, St. Louis, MO, USA), nestin, CD271 (NGFR, nerve growth factor receptor) (BD Biosciences, San Jose, CA, USA) and desmin antibodies with FITC-conjugated goat anti-mouse IgG (Dako, Carpinteria, CA, USA) were used only in LX-2 cell line. For intracellular detection of αSMA, GFAP, nestin and desmin cells were fixed with 1% paraformaldehyde, permeabilized with 1% Tween 20, and stained with specific antibody. At the analysis of Surface Epitope by FACS, cells were incubated with fluorescence-conjugated antibodies (1 μg-10^6 cells) at room temperature for 30 min. After washing twice with PBS 1×, cells were suspended in PBS and analyzed using the FACScalibur flow cytometer (BD Biosciences, San Jose, CA, USA). Ten thousand events were acquired and analyzed using the *CellQuest* software (BD Biosciences, San Jose, CA, USA). Nonspecific IgG of the corresponding class served as the negative control.

RNA isolation and cDNA synthesis

Total RNA was extracted from LX-2, HMBS and BM-MSC cells with the RNeasy Mini kit (Qiagen, Hilden, Germany) and stored at −80 °C. RNA was quantified using NanoVue systems (GE Healthcare, Piscataway, NJ, USA). RNA quality was checked by the integrity of the 28S and 18S rRNA bands displayed on a 1% agarose gel. Complementary DNA (cDNA) was synthesized from 2 μg of total RNA using a High Capacity cDNA Archive Kit (Applied Biosystems, Foster City, CA, USA) following the manufacturer's instructions.

qPCR analysis

The gene expression level of VIM (vimentin), annexin 5, COL1A1 (collagen, type I, alpha 1), NG2 (chondroitin sulfate proteoglycan 4), CD140b (PDGFRB, platelet-derived growth factor receptor, beta polypeptide), KDR (kinase insert domain receptor) and CD133 (AC133 or prominin 1) were assessed by quantitative real-time PCR in LX-2, HBMS and BM-MSC cells. In addition, the gene expression level of adiponectin (ADIPO) and alkaline phosphatase (ALPL) was also assessed in LX-2, HBMS and BM-MSC cells submitted or not to adipogenic and osteogenic differentiation induction. Quantitative real-time PCR (qPCR) (Bustin et al., 2009) was performed in a 15 μL volume for 40 cycles using universal cycling conditions (40 cycles of 95 °C for 15 s; 60 °C for 1 min) on an ABI Prism 7500 Sequence Detection System (Applied Biosystems, Foster City, CA, USA), using SYBR® Green PCR Master Mix, with efficiency values of PCR ranged from 1.22 to 0.93, and TaqMan® Universal PCR Master Mix (Applied Biosystems, Foster City, CA, USA). The SYBR primer concentration was 2.5 μM. Gene expression was normalized relative to the reference gene GAPDH and their relative expression in the different cell types was obtained as the protocol described previously by Albesiano et al. (2003). The cDNA was diluted 5 times in nuclease-free H_2O and was used in each qPCR reaction. The SYBR green primer sequences (forward/reverse) were: annexin 5, F-CAGCGGATGTTGGTGGTTCT and R-CCCCCATTTAAGTTCTCCAGC; CD140b, F-AACATCATCTGGTCTGCCTGC and R-TCAAACTCCTGCTCCTCCTC; NG2, F-GCTCGTGCTGTTCTCACACA and R-CCGTCACTCGGAAGAAGTGTC; KDR, F-ACTTCCTGACCTTGGAGCATC and R-AGGATATTTCGTGCCGCCAG; ADIPO, F-GGTGAGAAAGGAGATCCAGGT and R-CTTGGATTCCCGGAAAGCCTC; ALPL, F-CATCGCCTACCAGCTCATG and R-CTCGTCACTCTCATACTCCACA. All the TaqMan gene expression assay probes were inventoried, and hydrolysis probes ID assay were: COL1A1 — Hs00164004_m1, VIM — Hs00185584_m1 and CD133/prominin 1 — Hs00195682_m1.

Conventional PCR analysis

The cDNAs of LX-2 were used as template for PCR experiments. The primers used to amplify a 340 bp fragment of PPARγ (Peroxisome Proliferator-Activated Receptor Gamma) were 5′-GTTATGGGTGAAACT CTGGGAG-3′ (PPAR89 — forward) and 5′-GGAGATGCAGGCTCCACTTTG-3′ (PPAR429 — reverse); the primers used to amplify a 387 bp fragment of Osteopontin were 5′-CCATGAGAATTGCAGTGATTTGC-3′ (OST66 — forward) and 5′-GTCGTTCGAGTCAATGGAGTCC-3′ (OST388 — reverse) (Sigma-Aldrich, St. Louis, MO, USA). A 195 bp fragment of human β-actin was amplified as an endogen control (P1F: 5′-GCCCTGAGG-CACTCTTCC-3′; P1R: 5′-GCCCTGAGGCACTCTTCC-3′) (Sigma-Aldrich, St. Louis, MO, USA). All primers used in RT-PCR were located in different exons. The cDNA amplification reaction was performed in a 25 μL in the presence of 2 μL of cDNA, 10 mM dNTPs; 1 μL of Taq DNA polymerase (Amersham Bioscience, GE Healthcare, Piscataway, NJ, USA), 2.5 μL of 10× buffer of the respective enzyme (Amersham Bioscience, GE Healthcare, Piscataway, NJ, USA) and 1 μL of each primer (forward and reverse) to 10 pmol. The PCR reaction was performed in a thermocycler GeneAmp® PCR System 9700 (Applied Biosystems, Foster City, CA, USA) with the program: 95 °C for 2 min followed by 95 °C for 40 s, 60 °C for 40 s and 72 °C for 60 s for 35 cycles, with a final extension stage at 72 °C for 10 min. The PCR products were then separated by 1% agarose gel electrophoresis using PowerPac Basic™ (Bio-Rad, Benicia, CA, USA) and photographed under UV light using ImageQuant™ 350 (GE Healthcare, Piscataway, NJ, USA).

Determination of doubling time and population doubling level

LX-2, HBMS and BM-MSC cells were seeded (1.3×10^4 cells/cm^2) in 75 cm^2 tissue culture flasks (Corning, Corning, NY, USA) for 7 days with several medium changes until the cells had reached the maximum confluence. These analyses were made in duplicate. Living cells were trypsinized in trypsin-EDTA (Gibco — Invitrogen, Carlsbad, CA, USA) and counted using trypan-blue staining. Cell growth was monitored by determining the number of cumulative population doubling (PD) (Stenderup et al., 2003). This assay was repeated four times for all samples. The doubling time (DT) was calculated according to the formula, $DT = t*\ln(2)/\ln(A/Ao)$, where A is the cell number at time t (hours); Ao is the initial cell number (Legrier et al., 2007).

In vitro differentiation procedures

LX-2, HBMS and BM-MSC cells were assessed for their potential to induce differentiation into adipocytes and osteocytes. Cells from each source (1×10^4) were seeded on glass coverslips (GoldLab, Ribeirão Preto, SP, Brazil) in 24-well plates (Corning, Corning, NY, USA) and incubated with specific differentiation medium. For adipogenic differentiation, cells were grown in α-MEM (Gibco — Invitrogen, Carlsbad, CA, USA), supplemented with 15% FBS (Thermo Scientific HyClone, Logan, UT, USA) 1 mM of dexamethasone (Dex) (Sigma-Aldrich, St. Louis, MO, USA), 2.5 mg/mL of insulin and 0.5 mM isobutylmethylxanthine (Sigma-Aldrich, St. Louis, MO, USA). Sudan II-Scarlet staining (Oil Red O) (Sigma-Aldrich, St. Louis, MO, USA) was used to visualize lipid-rich vacuoles. To induce osteogenic differentiation, cells were grown in α-MEM (Gibco — Invitrogen, Carlsbad, CA, USA) supplemented with 7.5% FBS (Thermo Scientific HyClone, Logan, UT, USA), 0.1 mM of Dex (Sigma-Aldrich, St. Louis, MO, USA), 20 mM of ascorbic acid and 1 M β-glycerolphosphate (Sigma-Aldrich, St. Louis, MO, USA). Media were replaced every 3 days over 22 days and then cells were fixed using 4% paraformaldehyde (Sigma-Aldrich, St. Louis, MO, USA). After this period, cells were analyzed by von Kossa staining to identify calcium deposits. After washing with PBS, 1% silver nitrate (Sigma-Aldrich, St. Louis, MO, USA) was added and exposed to incandescent light bulb for 60 min and then washed with 5% sodium thiosulphate (Sigma-Aldrich, St. Louis, MO, USA) for 5 min. Control cells were kept in standard α-MEM (Gibco — Invitrogen, Carlsbad, CA, USA), with 15% FBS (Thermo Scientific HyClone, Logan, UT, USA) over the same period. Cells were analyzed with an AxioScope equipped with an AxioCam HR (Carl Zeiss, Jena, Germany).

Animals

Non-obese diabetic, severe combined immunodeficient (NOD/scid) female mice 8–10 weeks in age and weighing 25–30 g were provided by Biotery II of School of Pharmaceutical Sciences of Ribeirão Preto, University of São Paulo, Brazil. The mice were housed and cared in pathogen-free conditions. Experimental protocols were approved by the Ethics Committee for animal experiments of school of medicine of Ribeirão Preto, University of São Paulo, Brazil.

In vivo angiogenesis assay

The formation of vascular networks in vivo assay was evaluated by xenografting cells on NOD/scid female mice. Viable cells of each group consisting of LX-2 (2×10^6), HBMS (2×10^6), primary BM-MSCs (2×10^6), HUVEC (2×10^6), and a mixture of LX-2 + HUVEC or HBMS + HUVEC or primary BM-MSCs + HUVEC (ratio 1:1; [1×10^6]) were suspended in 200 μL of ice-cold Matrigel™ (BD Bioscience, San Jose, CA, USA). The mixture (Cell + Matrigel) was infused subcutaneously (sc) into the dorsal midline of 8–10 week old female NOD/scid mice using a 25 gauge needle attached to a 1 mL syringe (BD Bioscience, San Jose, CA, USA). Implants of Matrigel alone served as controls. One implant was injected per mouse and each experimental condition was performed in triplicate. One week later, all mice were sacrificed and the Matrigel plugs were removed for examination of vessel formation. In H&E-stained sections, we considered as blood vessel only tubular structures containing erythrocytes within the Matrigel.

In vivo tumorigenic assay

About 2×10^6 LX-2 cells were suspended in 200 μL of sterile PBS and injected sc into the dorsal midline of three mice (NOD/scid) using a 25 gauge needle attached to a 1 mL syringe (BD Bioscience, San Jose, CA, USA). The injected mice were monitored daily for the appearance of palpable tumors. Additionally, over 10^3 cells (LX-2) as a suspension in 100 μL of sterile PBS were injected intravenously (iv) into the caudal veins of three mice. As an experimental control, only PBS was injected iv and sc in female mice. After 21 days all animals were sacrificed for examination of tumor formation.

Histological examination

Tissue specimens (cells differentiated, tissues and Matrigel) were fixed in 3.7% formaldehyde for at least 24 h. Following, the specimens were dehydrated in serial ethanol/xilol dilutions, embedded in paraffin blocks and five-micron paraffin sections were stained with hematoxylin–eosin (H&E) for histopathologic analysis in light microscopy (AxioScope) equipped with an AxioCam HR (Carl Zeiss, Jena, Germany).

Statistical analysis

Assays were conducted at least in triplicate. To evaluate differences between cell lines after inducing adipogenic and osteogenic differentiation we used the Student-*t* test. Results are expressed as mean ± standard deviation (SD). We considered 0.05 as a significant value. All statistical analysis was done with GraphPad Prism 5.0 software (La Jolla, CA, USA).

Results

LX-2 cells display a BM-MSC-like phenotype

We analyzed surface markers and intracellular proteins, by flow cytometry. LX-2 cells expressed nestin (39.8 ± 1.25%) and α-smooth muscle actin (α-SMA, [86.3 ± 1%]), which is considered a classical marker of activated HSC. In addition, LX-2 cells were positive for neuronal markers and HSC markers such as glial fibrillary acidic protein (GFAP [44 ± 8.5%]) and neurotrophin p75NTR (CD271 [41.5 ± 1%]). However, LX-2 almost did not express desmin (2.9 ± 3.4%), a classical marker of activated rat HSC (Fig. 1). We also looked for evidence of markers on LX-2 cells that are characteristic of BM-MSC cells (Table 1). LX-2 cells are positive for BM-MSC markers such as CD44, CD29, CD90, CD73, HLA-I, CD49e, CD105, CD146, and CD166 and negative for hematopoietic markers CD14, CD45 and CD34, endothelial marker CD31 and HLA-class II polypeptides. The expression of vascular cell adhesion molecule-1 (VCAM-1/CD106) was low in primary BM-MSCs (12.44 ± 13.79%) and it was almost absent in LX-2 (2.2 ± 1.4%) and HBMS (1.82 ± 0.6%) cell lines.

The expression levels of some genes frequently expressed in BM-MSCs were analyzed by qPCR. We detected the expression of vimentin (a mesodermal marker) in similar levels in LX-2 and HBMS cells while primary BM-MSCs expressed 1.8-fold more. Annexin 5, a marker for mesenchymal progenitor cells, was expressed 2.2 times higher in primary BM-MSCs than in LX-2 and HBMS. The expression of collagen type IA, which is associated with tissue repair, was 10-fold or more lower in LX-2 and HBMS cells than in primary BM-MSCs. Expression of the pericyte marker, NG-2, was 1.1× higher in primary BM-MSCs than in LX-2 cells and HBMS cells. Moreover, large amounts of pericyte marker CD140b-mRNA were found on primary BM-MSCs and HBMS compared to LX-2. All three cellular types expressed very low and similar levels of endothelial marker KDR mRNA (Fig. 2), as positive control were used HUVEC cells (374.21 ± 1.4 expression units). The expression of CD133-mRNA, a marker for endothelial progenitor cells, was not detected in LX-2, HBMS and BM-MSCs, as positive control were used CD133+ cells after isolation from umbilical cord blood (96.34 ± 2.1 expression units).

The LX-2 cell line has a fibroblastic morphology and adheres to plastic surface (Fig. 3A). The growth kinetics of LX-2 and HBMS cell lines was similar, but variable when compared to primary BM-MSCs (Table 2). In general, during early (1st–3rd) passages primary BM-MSC cultures showed a low population doubling level (PD = 2.6 ± 1.07) and a high doubling time (DT = 94.4 ± 45.3 h). However the DT index increased up to quiescence, (1565.95 ± 858.31 h). In contrast, LX-2 cells and HMBS cells exhibited higher PD values, 3.18 ± 0.14 and 3.38 ± 0.1, respectively, and lower DT indices, 53.3 ± 2.3 h and 45.63 ± 5.8 h, respectively, than primary BM-MSCs.

After culturing with osteogenic or adipogenic differentiation-inductor medium, LX-2 cells present a similar pattern of differentiation as BM-MSCs, thereby confirming its BM-MSC-like character. The accumulation of calcium-rich mineralized matrix was evidenced by von Kossa staining (Figs. 3G, H and I) in LX-2, HMBS and BM-MSC cells after induction of differentiation. The expression levels of ALPL, osteogenic marker, by qPCR was 8.7-fold higher in primary BM-MSCs than in HBMS cells and 2× higher in HBMS than in LX-2 cells (Fig. 4A). In addition, we detected by conventional PCR the expression of Osteopontin, an osteogenic marker, in LX-2 differentiated in osteocytes (Fig. 4C). Adipogenic characteristics such as acquisition of intracellular lipid droplets evidenced by Sudan II/Scarlet staining (Figs. 3M, N and O), were confirmed in LX-2, HMBS and BM-MSC cells after induction of differentiation. We observed by qPCR that the expression of the adipogenic marker, ADIPO, was 6.6× higher in primary BM-MSCs than in HBMS cells and 3× higher in HBMS than in LX-2 cells (Fig. 4B). Besides, we detected by conventional PCR the expression of PPARγ, an adipogenic marker, in LX-2 differentiated in adipocytes (Fig. 4C).

Table 1
LX-2, HBMS and BM-MSC cells possess a similar immunophenotypic profile.

Surface markers	LX-2	HBMS	BM-MSCs
CD44	78.89 ± 0.23	77.44 ± 3.4	65.23 ± 16.68
CD29	81.5 ± 6	84.78 ± 0.45	81.80 ± 9.2
CD90	92.95 ± 1.15	97.89 ± 2.2	90.91 ± 10.75
CD73	51.9 ± 6.6	68.9 ± 3.2	65.81 ± 20.61
HLA class I	70.35 ± 4.4	79.3 ± 1.5	54.62 ± 27.81
CD 49e	81.8 ± 3.23	86.7 ± 1.92	70.30 ± 20.21
CD105	74.71 ± 17.15	91.01 ± 1.75	61.58 ± 15.51
CD146	37.41 ± 38.05	21.22 ± 13.6	44.61 ± 23.21
CD166	39 ± 34.8	87.9 ± 1.6	52.53 ± 22.15
CD14	0.38 ± 0.39	0.34 ± 0.2	1.18 ± 2.02
CD45	0.1 ± 0.1	2.05 ± 0.46	0.84 ± 1.67
CD34	0.38 ± 0.25	1.12 ± 0.25	0.42 ± 0.67
CD31	0.12 ± 0.04	0.15 ± 0.06	0.89 ± 1.26
HLA class II	0.75 ± 0.6	0.41 ± 0.22	0.47 ± 0.17
CD106	2.19 ± 1.4	1.82 ± 0.6	12.44 ± 13.79

LX-2 cells give support to blood vessel formation in vivo

To investigate whether LX-2 cells can give support to vasculogenesis in vivo, stimulating new blood vessel formation, the Matrigel plugs implant experiment was performed. We recovered the Matrigel plugs one week after implantation onto the backs of NOD/Scid mice together with endothelial cells. Histological sections revealed vessels with erythrocytes in implants containing LX-2 plus HUVEC cells, HBMS plus HUVEC cells and primary BM-MSCs plus HUVEC cells (Figs. 5D, F and H). Matrigels without cells were used as controls (Fig. 5A) — they did not elicit any vessel structures. We also noted that Matrigels with only HUVEC, LX-2, HBMS or primary BM-MSCs failed to form microvessels (Figs. 5B, C, E, G).

LX-2 cells do not induce tumorigenesis in vivo

The tumorigenic potential of the LX-2 cell line was examined in vivo. After 21 days, tumor structure was not observed in the NOD/Scid mice. The histopathological analysis showed absence of morphological changes in organs: spleen, liver, kidney, stomach, heart, lung and intestine of mice which received iv infusion of LX-2 (Figs. 6A–N) and muscle of mice which received sc infusion of LX-2 (Figs. 6O–P).

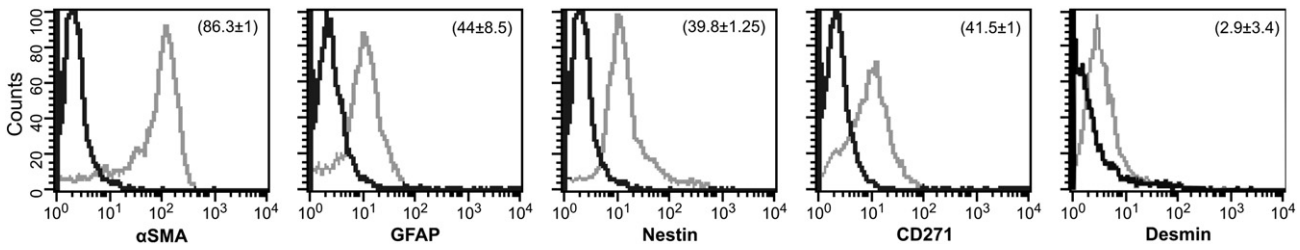

Fig. 1. LX-2 cells express the main proteins associated with human activated HSCs (αSMA, GFAP, Nestin, CD271 and desmin). Representative flow cytometry histograms. Y axis, % of cells; X axis, log of fluorescence intensity. Isotype controls are displayed in black, and samples incubated with specific antibodies are indicated in gray. Results are expressed as mean ± SD of three samples.

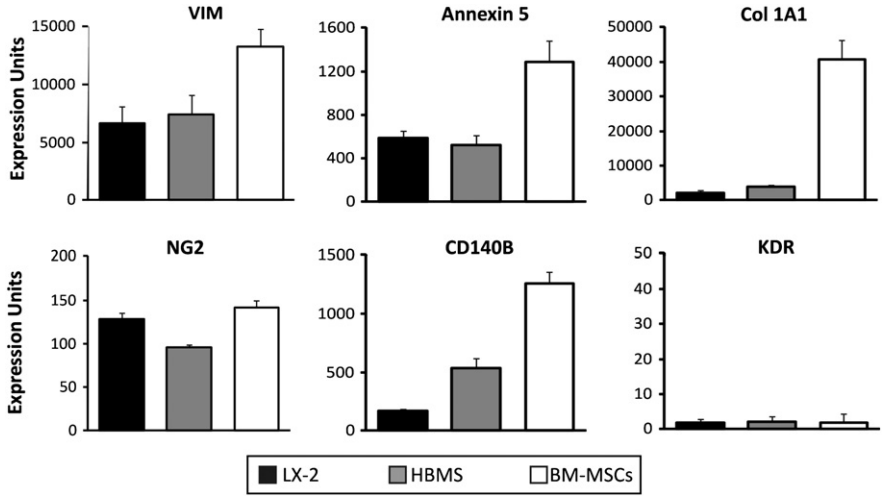

Fig. 2. LX-2, HBMS and primary BM-MSC cells exhibit similar levels of some transcripts associated with MSCs and pericytes. Comparative analyses of qPCR of mRNAs in LX-2, HBMS and BM-MSCs. Expressed genes included collagen type IA (Col 1A1) as well as markers for mesodermal origin (VIM), mesenchymal progenitor cells (annexin 5) and pericyte lineage (NG2 and CD140b). Expression of the endothelial marker, KDR, was at the limit of detection in all three cell lines. Gene expression was normalized relative to the reference gene GAPDH. Results are expressed as mean ± SD of three samples.

Discussion

At the present study we characterized human hepatic stellate cell line named as LX-2 cell line. This cell line allows the study of mechanisms of hepatic regeneration and the testing of antifibrotic drugs. The LX-2 cell line expresses many of the same genes and presents an immunophenotype that is similar to multipotent BM-MSCs, which have the capacity to differentiate into multilineage mesenchymal and angiogenic lineages that can form functional microvascular networks in vivo.

The identification of a hepatic stem cell line involved in liver regeneration is an important model for hepatic cellular therapy (Gaudio et al., 2009). Kordes et al. (2007) demonstrated, for the first time, that HSCs represent undifferentiated stem cells of the liver. HSCs are distinct — they can differentiate into either fibroblasts or myofibroblasts and they appear to play a fundamental role in repair and cicatrization in injured liver (Moreira, 2007; Reister et al., 2011; Senoo et al., 2010). The current knowledge of HSC behavior has been achieved through primary culture studies. However, different laboratories have established several HSC cell lines from mice (e.g., GRX, A7), rat (e.g., HSC-T6, HSC-PQ) and human beings (e.g., hTERT-HSC, LX-1) that provide stable and unlimited sources of cells (Herrmann et al., 2007). Because LX-2 cells were spontaneously immortalized during culturing, they are the most attractive HSC cell line.

The LX-2 cells cultured in our laboratory expressed GFAP and CD271. These proteins are considered early markers of HSC activation (Asahina et al., 2009; Carotti et al., 2008; Suzuki et al., 2008). The α-SMA expression has been used to identify activated HSCs that show a myofibroblastic phenotype (Asahina et al., 2009; Carpino et al., 2005) and in our LX-2 cell cultures we detected high proportion of α-SMA. Additionally, LX-2 also shows nestin reactivity that was reported as another marker of activated HSC by Niki et al. (1999). Previous works have demonstrated that desmin, a traditional activated HSC marker, is present in rodent but not in human HSC (Cassiman et al., 2002; Kiassov et al., 1995) and in accordance with these reports the protein-desmin showed a very low reactivity in LX-2 cultured in our laboratory. Thus, the phenotype of LX-2 cell line resembles human activated hepatic cells.

To detect the mesenchymal origin of LX-2 cells, we compared the expression levels of surface markers and genes related to mesenchymal stem cells, pericytes and endothelial progenitor cells, and we analyzed the growth rates of LX-2, HBMS and primary BM-MSCs. All three cellular populations showed a lack of hematopoietic and endothelial markers, which is consistent with the findings of others (Karp and Leng Teo, 2009). In sum, our results suggest that LX-2 cells are not closely related to either hematopoietic or endothelial lineages.

LX-2 cells were positive for HLA class-I markers and failed to express HLA-DR (one subclass of HLA class-II markers) as previously described for mesenchymal stem cells (Le Blanc et al., 2003). In addition, LX-2 cells expressed several markers in common with BM-MSCs (Deans and Moseley, 2000), including CD44, CD29, CD90, CD73, CD49e, CD105, CD146, and CD166. There is contention over the presence of the surface protein CD106/VCAM-1, which has been used to characterize all types of MSCs (Schieker et al., 2007). However, Liu and co-workers have speculated that CD106 is not a reliable surface marker for BM-MSCs and our results show that both LX-2 and HBMS cells hardly express this marker, suggesting that actually CD106 might not be a useful marker for BM-MSCs (Liu et al., 2008). Furthermore, we show that several genes usually expressed in BM-MSCs are also expressed in LX-2 cells. Transcripts that have been related with cell types of mesenchymal origin and mesenchymal progenitors cells [vimentin (Strutz et al., 1995) and annexin 5 (Brachvogel et al., 2005)], pericyte lineage [NG-2 (Ozerdem et al., 2002) and CD140b/PDGF-β (Tallquist et al., 2003)] were also expressed in LX-2 cells. As expected, transcripts of the endothelial marker — KDR (Bhattacharya et al., 2005), which show different roles in angiogenesis, were almost absent in our LX-2 cells. However, the in vitro study showed that the expression of KDR, also known as VEGFR-2 (vascular endothelial growth factor receptor 2) or FLK1 (fetal liver kinase-1), and VEGFR-1 [vascular endothelial growth factor receptor 1 or FLT1 (fms-related tyrosine kinase 1)], could be induced during activation of rat HSC, suggesting that the cellular targets of VEGF are not confined to endothelial cells (Ankoma-Sey et al., 1998). It has also been reported that in rat liver after necrosis, VEGF and its receptors derive from nonparenchymal as well as parenchymal cells (Ishikawa et al., 1999). In addition, transcripts of collagen type IA, which is associated with activated HSCs (Friedman, 2000) and liver fibrosis (Arthur et al., 1999; Brenner et al., 2000; Russo et al., 2006), were expressed in LX-2. Finally, CD133, a marker related to endothelial progenitor cells and hematopoietic stem cells in rats (Fujii et al., 2010; Kordes et al., 2007), was not expressed in LX-2, HBMS and BM-MSCs cultured in our laboratory.

Morphologies of cultured LX-2, HMBS cells and BM-MSCs adherent to plastic are typical of fibroblasts. However, LX-2 cells differed from BM-MSCs in culture medium constitutions; BM-MSCs require 15% FBS while LX-2 cells need only 2% FBS (Covas et al., 2008; Xu et al., 2005). LX-2 and HBMS cells showed similar growth rates whereas BM-MSCs

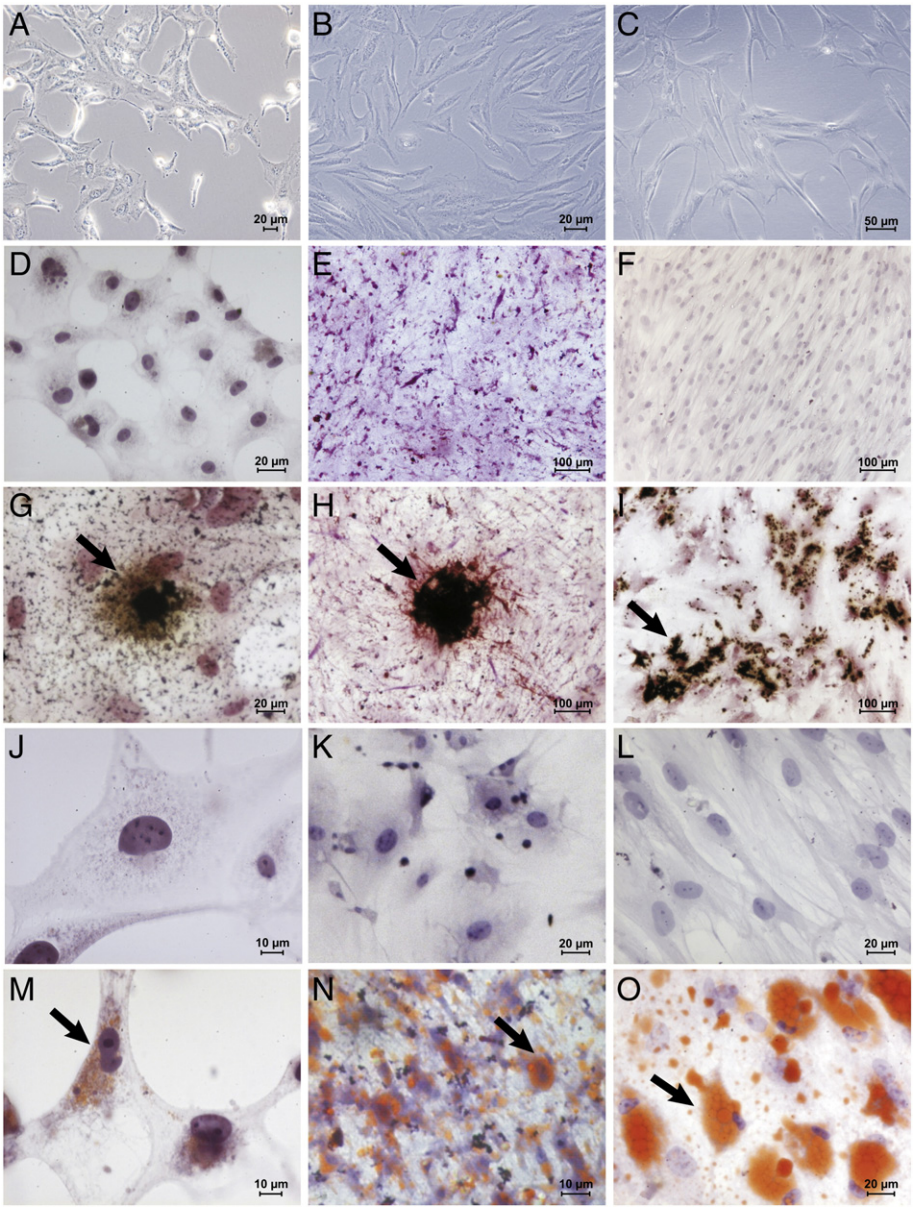

Fig. 3. LX-2, HBMS and primary BM-MSC cells have a fibroblastic morphology and presented in vitro multipotentiality including osteogenic and adipogenic differentiation. All cells, LX-2 (panel A), HBMS (panel B) and BM-MSCs (panel C), were plastic-adherent with a spindle-shaped morphology. Control cells cultured with standard medium were analyzed by von Kossa staining: LX-2 (panel D), HBMS (panel E) and BM-MSCs (panel F). Osteogenic induction was analyzed by von Kossa staining of calcium deposits: LX-2 (panel G), HBMS (panel H) and BM-MSCs (panel I). Control cells cultured with standard medium were analyzed by Sudan II/Scarlet staining: LX-2 (panel J), HBMS (panel K) and BM-MSCs (panel L). Adipogenic induction was analyzed by Sudan II/Scarlet staining of lipid vacuoles: LX-2 (panel M), HBMS (panel N) and BM-MSCs (panel O). The scale bars represent 10 μm (panels J and M), 20 μm (panels A, B, D, G, K, L, N and O), 50 μm (panel C) and 100 μm (panels E, F, H and I).

were slower. This difference could be attributed to the different origins of these cell types. In order to adapt to cell culture, BM-MSCs had to undergo subtle changes in vitro and their proliferative capacity has decreased with increasing passages (Kang et al., 2004). In contrast, LX-2 and HBMS cell lines have maintained their PD and DT indices under the same cultured conditions.

Table 2
Growth characteristics of LX-2, HBMS and BM-MSCs. Data presented is the mean of duplicate cultures.

Cells	Population doubling/passage	Population doubling time (hour)/passage
LX-2	3.18 ± 0.14	53.3 ± 2.3
HBMS	3.38 ± 0.1	45.63 ± 5.8
BM-MSCs[a]	2.6 ± 1.07	94.4 ± 45.3

[a] Cultured with standard fetal bovine serum.

LX-2 cells were able to differentiate into adipocytes and osteocytes, demonstrating similarly to the plasticity of HBMS and BM-MSC cells. The PPARγ, one of the key transcription factors for adipocyte differentiation, is expressed in the quiescent HSC (Miyahara et al., 2000), but its expression and activity are suppressed in activated HSC in vitro and in vivo (Galli et al., 2002), suggesting that PPARγ has been involved in the maintenance of a quiescent phenotype in HSC and the restoration of PPARγ in activated HSC induces a reversal of the morphological features of HSC to the quiescent phenotype (Yavrom et al., 2005). Our data about PPARγ mRNA expression confirm its depletion in activated HSC cell line (LX-2) and its presence in adipocyte-differentiated cellular LX-2 population.

Katritsis et al. (2005) demonstrated that BM-MSCs have the capacity to influence endothelial cell behavior and advance neoangiogenesis to help tissue repair in myocardial infarction. To that end, BM-MSCs promote endothelial cell migration and formation of

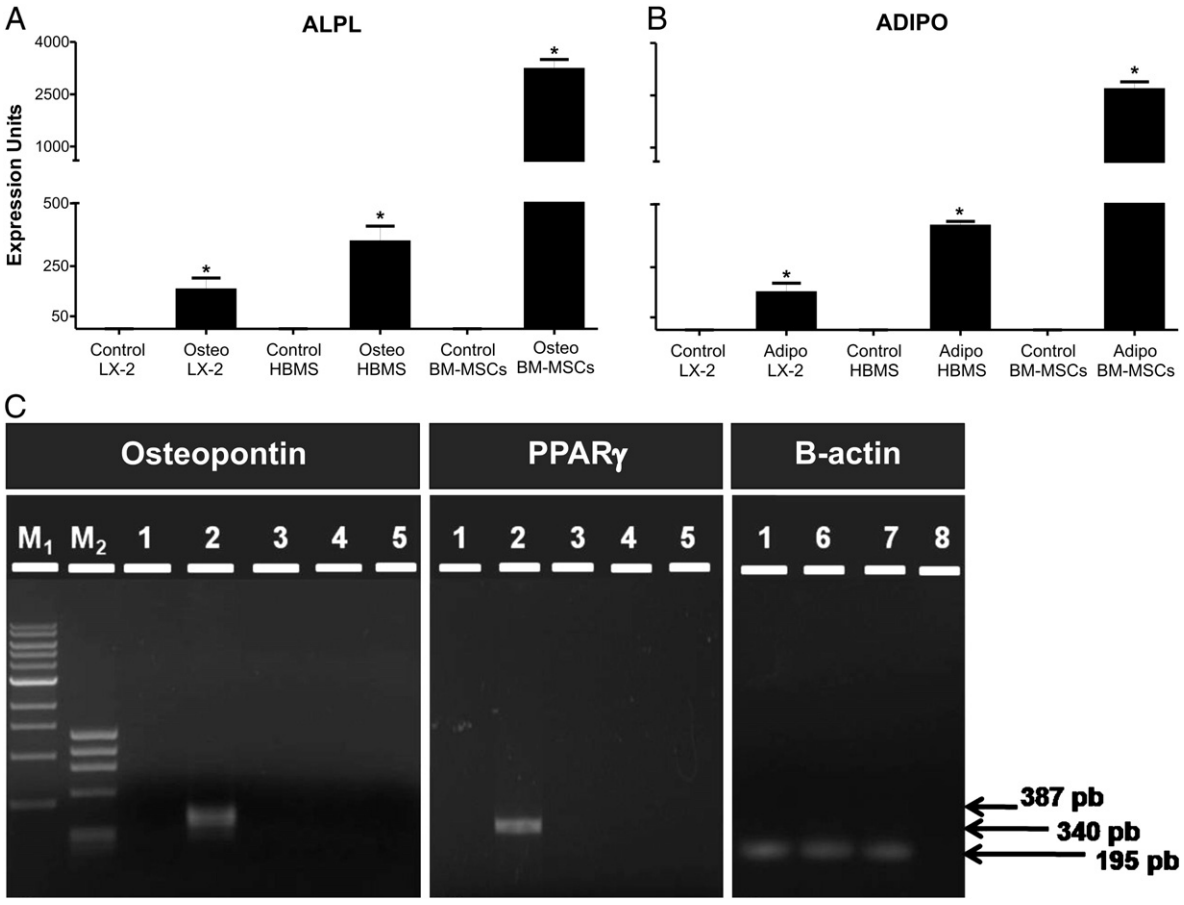

Fig. 4. Differentiated LX-2, HBMS and primary BM-MSC cells express transcripts associated with osteogenesis or adipogenesis. Cellular differentiation induction was analyzed by qPCR of mRNAs, LX-2, HBMS and BM-MSCs differentiated in osteocytes (OSTEO) have expressed ALPH gene (A), and LX-2, HBMS and BM-MSCs differentiated in adipocytes (ADIPO) have expressed ADIPO gene (B). Gene expression was normalized relative to the reference gene GAPDH. Results are expressed as mean ± SD of three samples. $^{*}p<0.05$ for differentiated cell related to control cell. Conventional PCR showed Osteopontin mRNA expression (387 pb) in OSTEO LX-2, PPARγ mRNA expression (340 pb) in ADIPO LX-2 and β-actin expression (195 pb) as endogenous control in LX-2 (C). Line M_1: 1 kb DNA ladder (fragments: 10.0; 8.0; 6.0; 5.0; 4.0; 3.0; 2.0; 1.5; 1.0; 0.5); Line M_2: ϕX174 ladder (fragments 1.3; 1.0; 0.8; 0.6; 0.2 kb); Line 1: control LX-2; Line 2: differentiated LX-2; Line 3: negative control of control LX-2; Line 4: negative control of differentiated LX-2 (negative control of reverse transcription reaction, did not add Multiscribe reverse transcriptase enzyme); Lines 5 and 8: negative control of PCR reaction; Line 6: OSTEO LX-2 — differentiated in osteocytes; Line 7: ADIPO LX-2 — differentiated in adipocytes. The size of amplified product is indicated by the black arrows.

tubular structures (Gruber et al., 2005). Accordingly, we employed an in vivo angiogenesis model to determine whether HSCs could help in the promotion of microvascular network formation in vivo in the same way as BM-MSCs. We found that LX-2 cells can support the formation of vascular networks when co-infused with HUVEC, thereby showing the same behavior of primary BM-MSC or HBMS cells. We detected

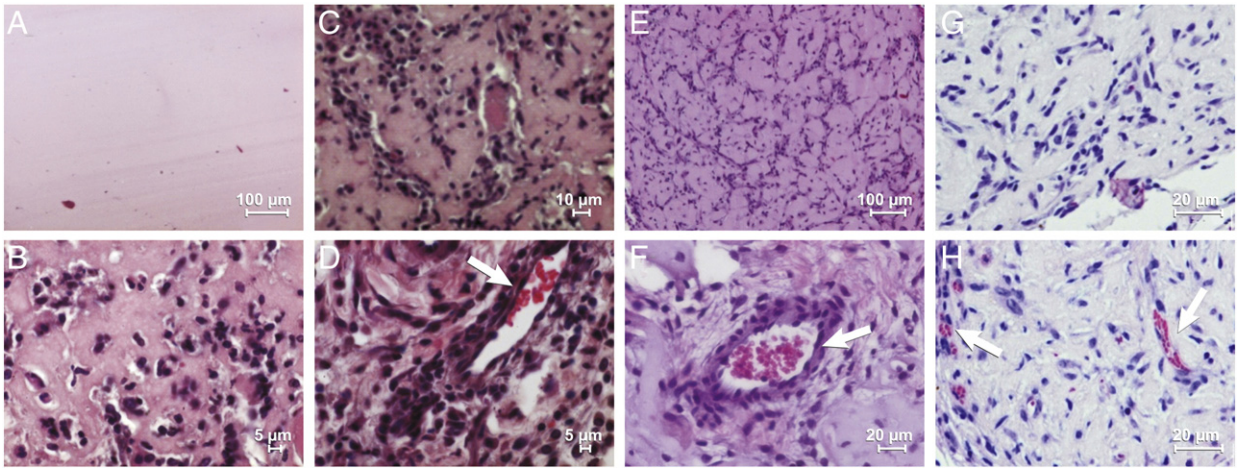

Fig. 5. LX-2, HBMS and primary BM-MSC cells contribute to the formation of neovascularization in vivo. After 7 days, H&E staining shows lumenal structures containing erythrocytes in Matrigel plugs with 1:1 ratios of HUVEC and LX-2 cells (D, arrow), HUVEC and HMBS cells (F, arrow), and HUVEC and BM-MSCs (H, arrow). Matrigels without cells were inert, and plugs were devoid of blood vessels (A). Matrigel plugs with HUVEC alone (B), LX-2 alone (C), HBMS alone (E) and BM-MSCs alone (G) failed to form microvessels. Images A and E are shown at 200× and images B, C, D, F, G, and H are shown at 400×. Scale bars represent 100 μm in panels A and E, 20 μm in panels F, G and H, 10 μm in panel C and 5 μm in panels B and D.

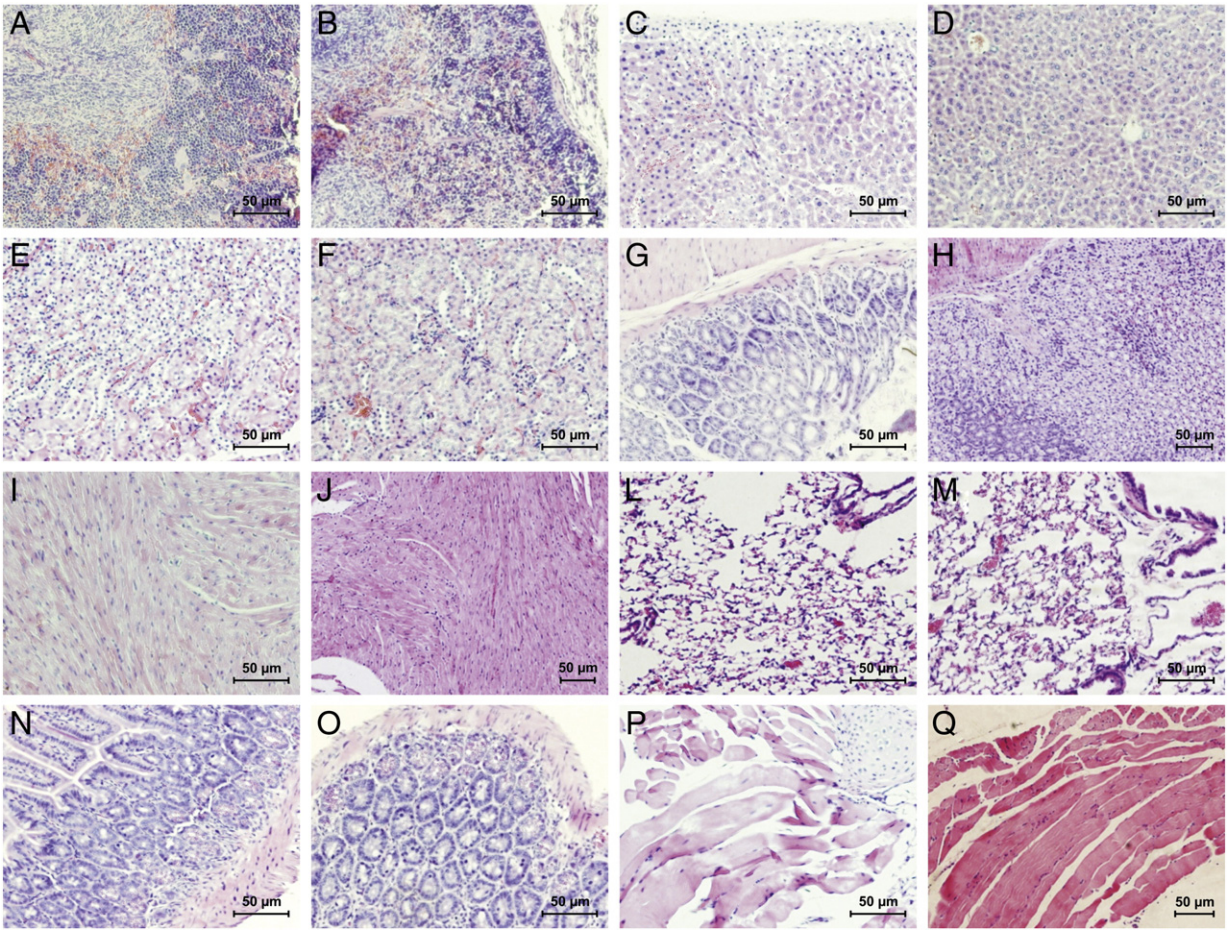

Fig. 6. LX-2 cells do not exhibit tumorigenic potential. LX-2 cells were infused intravenously or subcutaneously in NOD/scid mice and after 21 days the presence of tumor tissue was analyzed. The H&E staining of spleen (A–B), liver (C–D), kidney (E–F), stomach (G–H), heart (I–J), lung (L–M), and intestine (N–O) from control and injected mice, respectively did not show any indications of tumor formation. The muscle of control (P) and injected (Q) mice also showed normal tissues. The scale bars are 50 μm.

erythrocytes within newly formed blood vessels and demonstrated that they were functional and linked to the murine circulation.

BM-MSCs have very low immunogenicity, which promotes them to candidates for cell-based therapies (Bernardo et al., 2007; Choumerianou et al., 2008; Le Blanc and Ringden, 2005). Due to the similarities between LX-2 cells and BM-MSCs, we investigated whether LX-2 can generate tumors in vivo. In all treated mice no remarkable histopathological changes were observed after LX-2 transplants, suggesting that LX-2 cells may be as safe as BM-MSCs.

In conclusion, the present study demonstrates that LX-2 cell line population presents similarities with multipotent mesenchymal stem cells. This paper describes for the first time a wide in vitro and in vivo characterization of LX-2 cell line and their similarities with cultured BM-MSCs (primary and cell line). Thus, LX-2 can be a potential and more accessible cell source for stem cell-based therapy experimental models of acute or chronic liver injury and thus a new option for preclinical studies.

Acknowledgments

We would like to thank, Dr. Dario Campana (Department of Pediatrics, University of Tennessee College of Medicine, Memphis, TN) for kindly providing HBMS cell line. Also we thank Lucas E. B. Souza for providing technical support on Xenogen In Vivo Imaging System (IVIS). This work was supported by FAPESP, FINEP and INCTC.

References

Albesiano, E., et al., 2003. Activation-induced cytidine deaminase in chronic lymphocytic leukemia B cells: expression as multiple forms in a dynamic, variably sized fraction of the clone. Blood 102, 3333–3339.
Alison, M.R., et al., 2007. Application of liver stem cells for cell therapy. Seminars in Cell & Developmental Biology 18, 819–826.
Ankoma-Sey, V., et al., 1998. Coordinated induction of VEGF receptors in mesenchymal cell types during rat hepatic wound healing. Oncogene 17, 115–121.
Armulik, A., et al., 2005. Endothelial/pericyte interactions. Circulation Research 97, 512–523.
Arthur, M.J., et al., 1999. Tissue inhibitors of metalloproteinases: role in liver fibrosis and alcoholic liver disease. Alcoholism, Clinical and Experimental Research 23, 940–943.
Asahina, K., et al., 2009. Mesenchymal origin of hepatic stellate cells, submesothelial cells, and perivascular mesenchymal cells during mouse liver development. Hepatology 49, 998–1011.
Atzori, L., et al., 2009. Hepatic stellate cell: a star cell in the liver. The International Journal of Biochemistry & Cell Biology 41, 1639–1642.
Benyon, R.C., Arthur, M.J., 2001. Extracellular matrix degradation and the role of hepatic stellate cells. Seminars in Liver Disease 21, 373–384.
Bernardo, M.E., et al., 2007. Human bone marrow derived mesenchymal stem cells do not undergo transformation after long-term in vitro culture and do not exhibit telomere maintenance mechanisms. Cancer Research 67, 9142–9149.
Bhattacharya, R., et al., 2005. Regulatory role of dynamin-2 in VEGFR-2/KDR-mediated endothelial signaling. The FASEB Journal 19, 1692–1694.
Bordeaux-Rego, P., et al., 2010. Both interleukin-3 and interleukin-6 are necessary for better ex vivo expansion of CD133+ cells from umbilical cord blood. Stem Cells and Development 19, 413–422.
Brachvogel, B., et al., 2005. Perivascular cells expressing annexin A5 define a novel mesenchymal stem cell-like population with the capacity to differentiate into multiple mesenchymal lineages. Development 132, 2657–2668.
Brenner, D.A., et al., 2000. New aspects of hepatic fibrosis. Journal of Hepatology 32, 32–38.

Budny, T., et al., 2007. Morphologic features in the regenerating liver — a comparative intravital, lightmicroscopical and ultrastructural analysis with focus on hepatic stellate cells. Virchows Archiv 451, 781–791.
Bustin, S.A., et al., 2009. The MIQE guidelines: minimum information for publication of quantitative real-time PCR experiments. Clinical Chemistry 55, 611–622.
Carotti, S., et al., 2008. Glial fibrillary acidic protein as an early marker of hepatic stellate cell activation in chronic and posttransplant recurrent hepatitis C. Liver Transplantation 14, 806–814.
Carpino, G., et al., 2005. Alpha-SMA expression in hepatic stellate cells and quantitative analysis of hepatic fibrosis in cirrhosis and in recurrent chronic hepatitis after liver transplantation. Digestive and Liver Disease 37, 349–356.
Cassiman, D., et al., 2002. Hepatic stellate cell/myofibroblast subpopulations in fibrotic human and rat livers. Journal of Hepatology 36, 200–209.
Choumerianou, D.M., et al., 2008. Study of oncogenic transformation in ex vivo expanded mesenchymal cells, from paediatric bone marrow. Cell Proliferation 41, 909–922.
Covas, D.T., et al., 2008. Multipotent mesenchymal stromal cells obtained from diverse human tissues share functional properties and gene-expression profile with CD146+ perivascular cells and fibroblasts. Experimental Hematology 36, 642–654.
De Minicis, S., et al., 2007. Gene expression profiles during hepatic stellate cell activation in culture and in vivo. Gastroenterology 132, 1937–1946.
Deans, R.J., Moseley, A.B., 2000. Mesenchymal stem cells: biology and potential clinical uses. Experimental Hematology 28, 875–884.
Flohr, T.R., et al., 2009. The use of stem cells in liver disease. Current Opinion in Organ Transplantation 14, 64–71.
Friedman, S.L., 2000. Molecular regulation of hepatic fibrosis, an integrated cellular response to tissue injury. The Journal of Biological Chemistry 275, 2247–2250.
Friedman, S.L., 2008. Hepatic stellate cells: protean, multifunctional, and enigmatic cells of the liver. Physiological Reviews 88, 125–172.
Friedman, S.L., et al., 1985. Hepatic lipocytes: the principal collagen-producing cells of normal rat liver. Proceedings of the National Academy of Sciences of the United States of America 82, 8681–8685.
Fujii, T., et al., 2010. Mouse model of carbon tetrachloride induced liver fibrosis: histopathological changes and expression of CD133 and epidermal growth factor. BMC Gastroenterology 10, 79.
Galli, A., et al., 2002. Antidiabetic thiazolidinediones inhibit collagen synthesis and hepatic stellate cell activation in vivo and in vitro. Gastroenterology 122, 1924–1940.
Gaudio, E., et al., 2009. New insights into liver stem cells. Digestive and Liver Disease 41, 455–462.
Gruber, R., et al., 2005. Bone marrow stromal cells can provide a local environment that favors migration and formation of tubular structures of endothelial cells. Tissue Engineering 11, 896–903.
Herrmann, J., et al., 2007. Immortal hepatic stellate cell lines: useful tools to study hepatic stellate cell biology and function? Journal of Cellular and Molecular Medicine 11, 704–722.
Ishikawa, K., et al., 1999. Expressions of vascular endothelial growth factor in nonparenchymal as well as parenchymal cells in rat liver after necrosis. Biochemical and Biophysical Research Communications 254, 587–593.
Ito, T., Shibasaki, S., 1968. Electron microscopic study on the hepatic sinusoidal wall and the fat-storing cells in the normal human liver. Archivum Histologicum Japonicum 29, 137–192.
Kang, T.J., et al., 2004. Growth kinetics of human mesenchymal stem cells from bone marrow and umbilical cord blood. Acta Haematologica 112, 230–233.
Karp, J.M., Leng Teo, G.S., 2009. Mesenchymal stem cell homing: the devil is in the details. Cell Stem Cell 4, 206–216.
Katritsis, D.G., et al., 2005. Transcoronary transplantation of autologous mesenchymal stem cells and endothelial progenitors into infarcted human myocardium. Catheterization and Cardiovascular Interventions 65, 321–329.
Kiassov, A.P., et al., 1995. Desmin expressing nonhematopoietic liver cells during rat liver development: an immunohistochemical and morphometric study. Differentiation 59, 253–258.
Kordes, C., et al., 2007. CD133+ hepatic stellate cells are progenitor cells. Biochemical and Biophysical Research Communications 352, 410–417.
Le Blanc, K., Ringden, O., 2005. Immunobiology of human mesenchymal stem cells and future use in hematopoietic stem cell transplantation. Biology of Blood and Marrow Transplantation 11, 321–334.
Le Blanc, K., et al., 2003. HLA expression and immunologic properties of differentiated and undifferentiated mesenchymal stem cells. Experimental Hematology 31, 890–896.
Legrier, M.E., et al., 2007. Targeting protein translation in human non small cell lung cancer via combined MEK and mammalian target of rapamycin suppression. Cancer Research 67, 11300–11308.
Liu, F., et al., 2008. Changes in the expression of CD106, osteogenic genes, and transcription factors involved in the osteogenic differentiation of human bone marrow mesenchymal stem cells. Journal of Bone and Mineral Metabolism 26, 312–320.
Mann, J., Mann, D.A., 2009. Transcriptional regulation of hepatic stellate cells. Advanced Drug Delivery Reviews 61, 497–512.
McCuskey, R.S., 2008. The hepatic microvascular system in health and its response to toxicants. The Anatomical Record (Hoboken) 291, 661–671.
Mihara, K., et al., 2003. Development and functional characterization of human bone marrow mesenchymal cells immortalized by enforced expression of telomerase. British Journal of Haematology 120, 846–849.
Miyahara, T., et al., 2000. Peroxisome proliferator-activated receptors and hepatic stellate cell activation. The Journal of Biological Chemistry 275, 35715–35722.
Moreira, R.K., 2007. Hepatic stellate cells and liver fibrosis. Archives of Pathology & Laboratory Medicine 131, 1728–1734.
Niki, T., et al., 1999. Class VI intermediate filament protein nestin is induced during activation of rat hepatic stellate cells. Hepatology 29, 520–527.
Ozerdem, U., et al., 2002. NG2 proteoglycan expression by pericytes in pathological microvasculature. Microvascular Research 63, 129–134.
Reister, S., et al., 2011. The epigenetic regulation of stem cell factors in hepatic stellate cells. Stem Cells Dev.
Russo, F.P., et al., 2006. The bone marrow functionally contributes to liver fibrosis. Gastroenterology 130, 1807–1821.
Schieker, M., et al., 2007. Human mesenchymal stem cells at the single-cell level: simultaneous seven-colour immunofluorescence. Journal of Anatomy 210, 592–599.
Senoo, H., et al., 2010. Hepatic stellate cell (vitamin A-storing cell) and its relative past, present and future. Cell Biol Int. 34, 1247–1272.
Silva Jr., W.A., et al., 2003. The profile of gene expression of human marrow mesenchymal stem cells. Stem Cells 21, 661–669.
Stenderup, K., et al., 2003. Aging is associated with decreased maximal life span and accelerated senescence of bone marrow stromal cells. Bone 33, 919–926.
Strutz, F., et al., 1995. Identification and characterization of a fibroblast marker: FSP1. The Journal of Cell Biology 130, 393–405.
Suzuki, K., et al., 2008. p75 Neurotrophin receptor is a marker for precursors of stellate cells and portal fibroblasts in mouse fetal liver. Gastroenterology 135 (270–281), e3.
Tallquist, M.D., et al., 2003. Additive effects of PDGF receptor beta signaling pathways in vascular smooth muscle cell development. PLoS Biology 1, E52.
Wake, K., 1971. "Sternzellen" in the liver: perisinusoidal cells with special reference to storage of vitamin A. The American Journal of Anatomy 132, 429–462.
Xu, L., et al., 2005. Human hepatic stellate cell lines, LX-1 and LX-2: new tools for analysis of hepatic fibrosis. Gut 54, 142–151.
Yavrom, S., et al., 2005. Peroxisome proliferator-activated receptor gamma suppresses proximal alpha1(I) collagen promoter via inhibition of p300-facilitated NF-I binding to DNA in hepatic stellate cells. The Journal of Biological Chemistry 280, 40650–40659.
Zimmermann, A., 2004. Regulation of liver regeneration. Nephrology, Dialysis, Transplantation 19 (Suppl 4), iv6–iv10.